ELSEVIER

Journal of Fluorine Chemistry 71 (1995) 123–129

JOURNAL OF FLUORINE CHEMISTRY

Characterization of the adducts $WF_6 \cdot py$ and $WF_6 \cdot 2py$ (py = pyridine): crystal structure of $WF_6 \cdot 2py$

L. Arnaudet, R. Bougon *, B. Buu, M. Lance, M. Nierlich, P. Thuéry, J. Vigner

SCM, URA CNRS 331, CEA, Centre d'Etudes de Saclay, 91191 Gif-sur-Yvette, France

Received 27 February 1994; accepted 7 May 1994

Abstract

Adducts of tungsten(VI), i.e. $WF_6 \cdot py$ and $WF_6 \cdot 2py$ (py = pyridine) have been characterized by X-ray diffraction data and vibrational spectroscopy. Solutions of these adducts in CD_2Cl_2 have also been studied by ^{19}F, ^{1}H and ^{13}C NMR spectroscopy. The ^{19}F NMR spectra, recorded at 193 K for $WF_6 \cdot 2py$ and at 140 K for $WF_6 \cdot py$, were both of the A_4X_2 type. The geometry of the coordination polyhedron of the W atom in $WF_6 \cdot py$ could not be determined by X-ray diffraction methods. However, the 1:2:4 arrangement of the ligands indicated by the ^{19}F NMR data corresponds to a monocapped trigonal prism. The approximate values of the activation energy for internal fluorine exchange calculated from the ^{19}F NMR data are 143 and 47 kJ mol^{-1} for $WF_6 \cdot 2py$ and $WF_6 \cdot py$, respectively. The crystal structure of $WF_6 \cdot 2py$, as determined by X-ray diffraction methods, is in agreement with the ^{19}F NMR data. In this adduct, the tungsten atom is surrounded by an undecahedron of ligands derived from a trigonal prism by the capping of two square faces (2:2:4 ligand arrangement) with the nitrogen atoms of the organic ligand occupying the capping sites. The crystal system, space group, unit cell parameters, and R factor are as follows: orthorhombic, *Pnma* (No. 62), $a = 14.274(2)$ Å, $b = 13.335(2)$ Å, $c = 6.497(2)$ Å, $V = 1236.8(8)$ Å^3, $Z = 4$, $R = 0.020$.

Keywords: Tungsten hexafluoride; Pyridine; Tungsten (VI) fluoro-adducts; Heptacoordination; Octacoordination

1. Introduction

Several geometries are observed for the coordination polyhedron of a central atom with a coordination number (CN) equal to seven or eight. Depending on the nature of the ligands, the most common geometries for CN seven are the capped trigonal prism and the pentagonal bipyramid, and for CN eight the square antiprism and the triangular dodecahedron [1].

Among the adducts previously obtained with tungsten(VI) fluoride and oxide fluorides in combination with uni- or bi-dentate nitrogen bases, pentagonal bipyramid and capped trigonal prism arrangements have been found for $WOF_4 \cdot 2py$ and $WF_6 \cdot$F-py, respectively [2,3]. Still for CN seven, the $[WF_7]^-$ ion in complexes derived from the reaction of bipy with WF_6 was also found to have a capped trigonal prism arrangement of ligands [4,5]. Only one type of arrangement has been found in this class of compounds for CN eight: the triangular dodecahedron in the cation $WF_4(bipy)_2]^{2+}$ [4,5] (py = pyridine, F-py = 2-fluoropyridine, bipy = 2,2′-bipyridyl).

The adducts $WF_6 \cdot py$ and $WF_6 \cdot 2py$, which were first prepared by Tebbe and Muetterties [6], were thought to be good representatives of CN seven- and CN eight-type adducts. The fact that the coordination of the central atom in these two adducts with different CN values is achieved with the same ligands makes structural comparison more meaningful. As the structures of $WF_6 \cdot py$ and $WF_6 \cdot 2py$ were still unknown, the main purpose of the work reported here was to determine their structural characteristics.

2. Experimental details

2.1. NMR and Raman spectral measurements

The experimental procedures, material, apparatus and instrumentation were as described previously [7,8]. The NMR spectra were recorded on a Bruker model AC-200 spectrometer at 200.13, 188.3 and 50.32 MHz

* Corresponding author.

SSDI 0022-1139(94)03160-6

for ^{1}H, ^{19}F and ^{13}C, respectively. Samples were referenced externally with respect to $Si(CH_3)_4$ or $CFCl_3$, with positive shifts being downfield from the standards. A mixture of $CHClF_2$ and CD_2Cl_2 in a 80:20 molar ratio was used as the solvent at temperatures lower than that permitted by CD_2Cl_2 alone (ca. 193 K). Thick-walled (1.4 mm) NMR tubes of 5-mm o.d. were used for the $CHClF_2$-containing solutions. The 514.5-nm exciting line of an Ar ion model 2016 Spectra Physics laser was used to record the Raman spectra. In order to prevent decomposition of the adducts by the laser beam, the spectra were recorded with the samples mounted in an unsilvered Pyrex dewar filled with liquid nitrogen.

2.2. Preparation of $WF_6 \cdot 2py$ and $WF_6 \cdot py$

The adduct $WF_6 \cdot 2py$ was prepared from the reaction of 4.55 mmol of pyridine in 3 cm^3 of CH_2Cl_2 into which 1.48 mmol of WF_6 was added by condensation at −196 °C. A white precipitate resulted from warming of the mixture to ambient temperature. Most of the solvent and excess pyridine were removed by decantation at this temperature. The product was finally dried in a dynamic vacuum at −20 °C for ca. 0.5 h, and at ambient temperature for a few minutes. Analysis: Calc. for $WF_6 \cdot 2py$: W, 40.31; F, 24.99; C, 26.34; H, 2.21; N, 6.14%. Found: W, 40.41; F, 24.86; C, 26.14; H, 2.32; N, 6.05%. This adduct was also obtained by using pyridine as the solvent. The adduct $WF_6 \cdot py$ was prepared as described above for $WF_6 \cdot 2py$, but using stoichiometric amounts (typically 2 mmol) of pyridine and WF_6 in CH_2Cl_2. Analysis: Calc. for $WF_6 \cdot py$: W, 48.77; F, 30.24; C, 15.93; H, 1.34; N, 3.42%. Found: W, 48.50; F, 30.15; C, 15.92; H, 1.24; N. 3.62%.

Both adducts were very sensitive towards moisture. They were stable at ambient temperature when kept in glass ampules sealed under vacuum. However, they

Table 1
X-Ray powder diffraction data for $WF_6 \cdot py$ and $WF_6 \cdot 2py$

$WF_6 \cdot py$ [a]				$WF_6 \cdot 2py$ [b]	
d (Å)		Intens. [c]	hkl	d (Å)	Intens. [c]
Obs.	Calc.				
7.37	7.38	ms	110	6.676	s
5.98	5.99	s	−111	6.103	vs
5.37	5.42	ms	200	5.534	m
4.583	4.572	m	120	5.007	m
4.111	4.137	ms	021	4.857	ms
3.686	3.691	s	220	4.227	m
3.587	3.612	m	300	3.782	w
3.386	3.401	vw	310	3.705	vvw
3.189	3.211	m	130	3.608	m
3.056	3.049	vw	031	3.470	m
2.976	2.963	mw	112	3.330	m
2.700	2.709	mw	400	3.264	vvw
2.579	2.592	vw	202	3.061	m,br
2.520	2.521	mw	040	2.938	w
2.443	2.456	vw	140	2.846	mw
2.375	2.387	mw	420	2.773	m
2.268	2.267	m,br	141	2.653	mw
	2.273		−502	2.561	w
2.167	2.167	vvw	500	2.499	mw
			331	2.421	mw
2.125	2.13	vw	312	2.336	vvw
2.067	2.067	m	340	2.285	vvw
1.983	1.983	w	150	2.238	m
1.937	1.934	mw	−304	2.184	vvw
1.875	1.871	w	−114	2.113	ms
1.848	1.846	w	−442	2.074	w
1.808	1.806	mw	600		

[a] The pattern is indexed for a monoclinic cell with parameters: $a = 11.693(9)$ Å, $b = 10.086(4)$ Å, $c = 7.807(2)$ Å, $\beta = 112.06(6)°$.
[b] See text.
[c] Abbreviations used: br, broad; v, very; s, strong; m, medium; w, weak.

Table 2
Crystallographic data for $WF_6 \cdot 2py$

Crystal data	
Formula	$C_{10}H_{10}N_2F_6W$
Formula weight	456.05
Crystal size (mm)	0.25 × 0.25 × 0.20
Crystal colour	colourless
Crystal system	orthorhombic
Space group	*Pnma* (No. 62)
a (Å)	14.274(2)
b (Å)	13.335(2)
c (Å)	6.497(2)
V (Å^3)	1236.8(8)
Z	4
ρ_{calc} (g cm^{-3})	2.449
μ(Mo Kα) (cm^{-1})	96.02
Data collection	
Diffractometer	CAD 4 Enraf-Nonius
Monochromator	graphite
Radiation	Mo Kα ($\lambda = 0.71073$ Å)
T (K)	293
θ limits (°)	1, 25
Scan type	$\omega/2\theta$
Scan width	$0.80 + 0.35 \tan \theta$
Range abs. transm.	0.99, 0.77
Range of $h\ k\ l$	$0 \le h \le 16$, $0 \le k \le 15$, $0 \le l \le 7$
Reflections collected	
total	1351
unique	1136
Kept for refinement ($I > 3\sigma(I)$)	835
Number of parameters varied	91
Minimized function	$\Sigma w[\|F_o\| - \|F_c\|]^2$
Weighting scheme	unit weight for all reflections
$R(F) = \Sigma\|\|F_o\| - \|F_c\|\|/\Sigma\|F_o\|$	0.020
$Rw(F) = [\Sigma w[\|F_o\| - \|F_c\|]^2/\Sigma w[\|F_o\|]^2]^{1/2}$	0.027
$(\Delta/\sigma)_{max}$	0.01
Computer used	VAX 4200
Computing programs	MolEN [10], ORTEP [11], SYBYL [13]

Table 3
Positional and thermal parameters for $WF_6 \cdot 2py$ and their estimated standard deviations

Atom	x	y	z	B (Å²) [a]
W	0.08906(3)	0.250	0.17988(6)	2.720(7)
F(1)	0.0326(4)	0.250	0.4422(9)	3.0(1)
F(2)	0.2086(4)	0.250	0.302(1)	3.2(1)
F(3)	0.1444(4)	0.1647(4)	−0.0197(7)	4.6(1)
F(4)	−0.0115(3)	0.1645(4)	0.1034(7)	4.4(1)
N	0.1143(4)	0.0932(5)	0.333(1)	2.9(1)
C(1)	0.0943(6)	0.0075(6)	0.233(1)	3.7(2)
C(2)	0.1084(6)	−0.0856(6)	0.321(1)	4.5(2)
C(3)	0.1418(6)	−0.0902(7)	0.521(1)	4.1(2)
C(4)	0.1608(6)	−0.0027(6)	0.623(1)	3.6(2)
C(5)	0.1469(5)	0.0866(6)	0.529(1)	3.1(2)

[a] Atoms were refined anisotropically. $B = 4/3\Sigma_i\Sigma_j \beta_{ij} \mathbf{a}_i \mathbf{a}_j$.

exhibited weak dissociation pressures at this temperature since they sublimed under dynamic vacuum.

2.3. Single-crystal X-ray diffraction studies

Crystals of $WF_6 \cdot 2py$ suitable for structure determination, obtained from CH_2Cl_2 solution, were selected in the dry box, coated with Kel-F oil and sealed inside glass capillaries of 0.5 mm diameter. Curiously, the reproducible X-ray powder pattern obtained for samples of $WF_6 \cdot 2py$ which had not been recrystallized in CH_2Cl_2 did not match the pattern calculated from the X-ray single-crystal study. Since significant departures from the theoretical composition are ruled out, this different pattern (listed in Table 1) is most likely due to a different crystal form of $WF_6 \cdot 2py$.

Sublimation of $WF_6 \cdot py$ under vacuum gave a mixture of the two adducts, and crystallization from CH_2Cl_2 solution failed to yield crystals suitable for structure determination. However, the cell parameters were determined from the few reflections observed for one of the crystals before its total decay, and the X-ray powder pattern could be indexed with these parameters (see Table 1).

The cell parameters of $WF_6 \cdot 2py$ were determined by least-squares refinement of the setting angles of 25 randomly selected reflections with θ between 8° and 12°. Three standard reflections were measured each hour to monitor the crystal decay (0.1% h^{-1}) and a linear correction was made. The data were corrected for Lorentz polarization effects and absorption using empirical corrections [9]. A summary of the X-ray data collection parameters and structural refinement is given in Table 2. The position of the W atom was determined by the heavy-atom method and the positions of other non-H atoms from subsequent difference-Fourier maps. Hydrogen atoms were included using a riding model (C−H:0.95 Å; B:6 Å²). The refinement was performed by a full-matrix least-squares procedure with anisotropic thermal parameters for all non-H atoms. The residual peaks on the final difference map were found to be smaller than 0.49 e $Å^{-3}$. The atomic scattering factors including anomalous dispersion terms were taken from *International Tables for X-ray Crystallography* [12].

3. Results and discussion

3.1. Syntheses

The reaction of WF_6 with py in stoichiometric amounts led to the adduct $WF_6 \cdot py$. In the presence of excess py, or in neat py, the adduct $WF_6 \cdot 2py$ was obtained. No indications were found for the formation of an adduct with a higher py/WF_6 molar ratio. The 1:1

Table 4
Selected bond lengths (Å) and angles (°) for $WF_6 \cdot 2py$ [a]

Bond	Length	Bond	Length	Bond	Length
W–F(1)	1.885(6)	W–N	2.344(6)	C(2)–C(3)	1.38(1)
W–F(2)	1.883(6)	N–C(1)	1.34(1)	C(3)–C(4)	1.37(1)
W–F(3)	1.898(5)	N–C(5)	1.36(1)	C(4)–C(5)	1.36(1)
W–F(4)	1.900(5)	C(1)–C(2)	1.38(1)		
Bonds	**Angle**	**Bonds**	**Angle**	**Bonds**	**Angle**
F(1)–W–F(2)	90.3(3)	F(3)–W–F(4^i)	119.7(2)	W–N–C(1)	121.4(5)
F(1)–W–F(3)	142.7(2)	F(3)–W–F(4)	77.1(2)	W–N–C(5)	120.5(6)
F(1)–W–F(4)	85.0(2)	F(3)–W–N	72.0(2)	C(1)–N–C(5)	118.1(7)
F(1)–W–N	71.5(2)	F(3)–W–N^i	139.6(2)	N–C(1)–C(2)	122.2(8)
F(2)–W–F(3)	84.9(2)	F(4)–W–F(4^i)	73.7(3)	C(1)–C(2)–C(3)	118.6(8)
F(2)–W–F(4)	142.7(2)	F(4)–W–N^i	139.7(2)	C(2)–C(3)–C(4)	118.9(9)
F(2)–W–N	71.4(2)	F(4)–W–N	72.1(2)	C(3)–C(4)–C(5)	120.1(8)
F(3)–W–F(3^i)	73.7(3)	N–W–N^i	126.3(3)	N–C(5)–C(4)	122.1(8)

[a] Symmetry code: (^{i}) x, $1/2-y$, z.

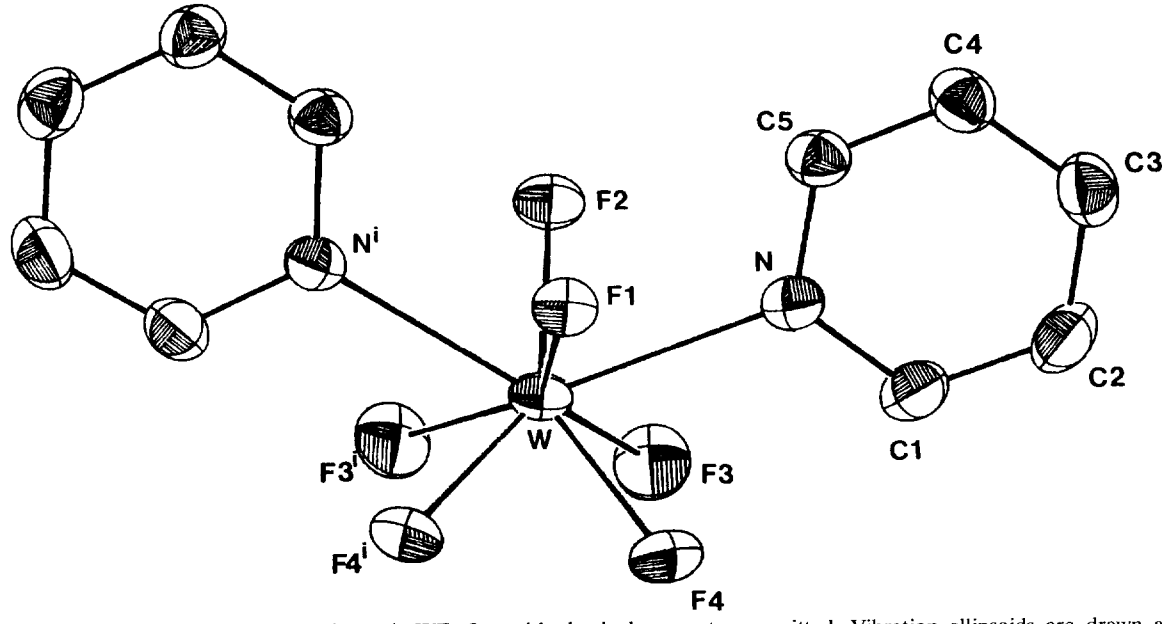

Fig. 1. ORTEP [11] drawing of the molecular unit $WF_6 \cdot 2py$ with the hydrogen atoms omitted. Vibration ellipsoids are drawn at the 30% probability level (symmetry code for i: x, $1/2-y$, z).

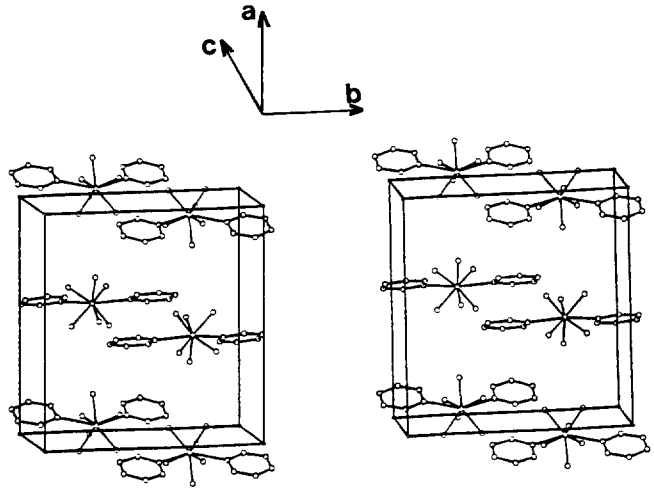

Fig. 2. Stereoscopic view of the structure in the unit cell of $WF_6 \cdot 2py$.

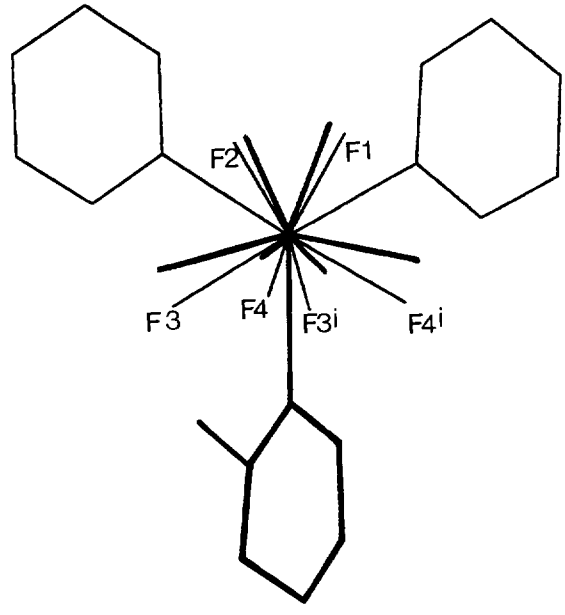

Fig. 3. Combined SYBYL [13] drawings of $WF_6 \cdot 2py$, —, and $WF_6 \cdot F\text{-}py$, ▬. The labelling corresponds to $WF_6 \cdot 2py$.

adduct dissociated under dynamic vacuum at ambient temperature, and a crystalline deposit with a composition intermediate between those of the 1:1 and 1:2 adducts was recovered in the cold trap. Dissociation of the 1:2 adduct was observed to proceed more slowly under the same conditions. The 1:2 adduct was converted into the 1:1 adduct by addition of WF_6 to the CH_2Cl_2 solutions. These observations and the preparations suggest that equilibria such as those depicted in Eqs. (1) and (2) might take place.

$$WF_6 + py \rightleftharpoons WF_6 \cdot py \quad (1)$$

$$WF_6 \cdot py + py \rightleftharpoons WF_6 \cdot 2py \quad (2)$$

However, unlike $WOF_4 \cdot 2py$ [2] and $WF_6 \cdot F\text{-}py$ [3], no indications were found by NMR spectroscopy for the dissociation of the adducts in CH_2Cl_2 up to ambient temperature. Consequently these hypothetical equilibria must be shifted very much to the right at ambient temperature.

3.2. Crystal structure

The positional and thermal parameters for $WF_6 \cdot 2py$ are given in Table 3, and selected bond lengths and angles are presented in Table 4. A drawing of the molecular structure and a stereoscopic view of the unit cell are shown in Figs. 1 and 2, respectively. The tungsten

Table 5
^1H and ^{13}C NMR data[a] for solutions of $WF_6 \cdot py$ and $WF_6 \cdot 2py$ in CD_2Cl_2, and a comparison with those of py

	^1H								
	$\delta_{1/5}$	$\delta_{2/4}$	δ_3	$J_{1,2/4,5}$	$J_{1,3/3,5}$	$J_{1,4/2,5}$	$J_{1,5}$	$J_{2,3/3,4}$	$J_{2,4}$
py	8.58	7.25	7.65	4.9	1.8	1.0	0.0	7.7	1.4
$WF_6 \cdot 2py$	9.12	7.60	8.02	5.9	1.5	0.7	0.9	7.6	1.7
$WF_6 \cdot py$	9.17	7.75	8.19	6.3	1.4	0.5	0.8	7.6	1.9
	^{13}C								
	$\delta_{1/5}$	$\delta_{2/4}$	δ_3	$J_{C1,H1}$	$J_{C2,H2}$	$J_{C3,H3}$			
py	150.28	124.05	136.13	179.0	168.9	161.7			
$WF_6 \cdot 2py$	146.12	125.42	139.85	186.1	167.5	164.8			
$WF_6 \cdot py$	146.10	126.40	142.27	184.7	168.8	165.6			

[a] Chemical shifts δ in ppm from TMS; coupling constants J in Hz; subscripts 1 to 5 refer to hydrogen or carbon positions, with (1 and 5), (2 and 4) and 3 indicating positions *ortho*, *meta* and *para* to the nitrogen atom, respectively. The ^1H NMR spectra were analyzed as an ABB'XX' spin system using the program PANIC from Bruker. The assignment of the lines of the ^{13}C spectra was deduced from the 2D correlation spectra, and the ^{13}C–^1H coupling constants were determined by the 2D sequence HETJRES provided by Bruker.

atom is in a bicapped trigonal prismatic environment. The planes [F(1), F(4), F(4^i)] and [F(2), F(3), F(3^i)] (see Fig. 1), which are perpendicular to the symmetry plane of the molecular unit, are roughly parallel [dihedral angle 7.7(7)°]. Departure from perfect parallelism is characterized by an inter-plane distance slightly longer on the side where the two pyridines are located. The W atom and the capping N atoms are at virtually equal distances from these two planes (W:1.24 Å; N: 1.31 Å).

In the absence of X-ray-based structural data for $WF_6 \cdot py$, it is interesting to compare the molecular arrangements of $WF_6 \cdot 2py$ and $WF_6 \cdot$ F-py [3]. The close structural analogy which was found between $WOF_4 \cdot py$ and $WOF_4 \cdot$ F-py [2,3] together with the ^{19}F NMR data obtained for $WF_6 \cdot py$ (see below), permits such a comparison. The geometry of the trigonal prism having F atoms as vertices is distorted either by one ($WF_6 \cdot$ F-py) or two ($WF_6 \cdot 2py$) capping ligands. Fixing both W atoms at the same point and superimposing the plane [F(1), W, F(2)] of $WF_6 \cdot 2py$ with the corresponding plane in $WF_6 \cdot$ F-py enables the difference between the two sets of bond angles [13] to be visualized (see Fig. 3). The distortion originates from the non-bonded repulsive interaction between the N atom(s) and the four adjacent F atoms. As a consequence, for $WF_6 \cdot 2py$ the pyramids having W as the common vertex and the two capped faces [F(1), F(2), F(3), F(4)] and [F(1), F(2), F(3^i), F(4^i)] as the base are squashed along the N–W and N^i–W axis, respectively. For $WF_6 \cdot$ F-py, the pyramid having W as the vertex and the capped face (homologue of [F(3), F(4), F(3^i), F(4^i)]) as the base is squashed along the axis joining W to the midpoint of F(1)–F(2).

3.3. NMR studies

NMR spectra were recorded for solutions of the adducts in CD_2Cl_2 or in a $CD_2Cl_2/CHClF_2$ mixture. The ^1H and ^{13}C NMR data are shown in Table 5 together with those for pyridine. No significant changes in the ^1H spectra were brought about by temperature variation in the 298–193 K range. The ^1H NMR spectra of the adducts were similar to those of pyridine, but shifted to higher frequency with the shifts for the 1:1 adduct being more pronounced. The ^{19}F spectrum of $WF_6 \cdot 2py$ is of the A_4X_2 type. At 193 K, it consisted of a triplet at $\delta = 124$ ppm and a quintet at $\delta = 75$ ppm with $J_{FF} = 88$ Hz. The triplet corresponds to the four equivalent fluorine atoms of one square face of a trigonal prism and the quintet to the two equivalent fluorine atoms of the edge opposite to this face. At 213 K, the multiplet structures were no longer observed, and at 243 K and above only one broad line was observed ($\delta = 120$ ppm, $\Delta_{1/2}$ (full width at half the maximum intensity) = 4227 Hz at 243 K, and $\delta = 116.7$ ppm, $\Delta_{1/2} = 300$ Hz at 273 K). The ^{19}F NMR spectrum of $WF_6 \cdot py$ recorded at 140 K was also found to be of the A_4X_2 type with a triplet at $\delta = 145.5$ ppm and a quintet (not fully resolved) at $\delta = 207.4$ ppm with $J_{FF} = 48$ Hz. At 143 K the multiplet components were coalesced, and at 203 K, consistent with a rapid intramolecular rearrangement, only one broad line was observed at $\delta = 166$ ppm, $\Delta_{1/2} = 2680$ Hz. As expected from the electron density conferred on the W atom in $WF_6 \cdot 2py$, the shift to lower frequency observed for all the F atoms indicates an increase in their shielding compared to those of WF_6. Furthermore, the set of four atoms [F(3), F(4), F(3^i), F(4^i)] (see labelling in Fig. 1) is less shielded than the set [F(1), F(2)]. The chemical shift of the broad average signal observed for $WF_6 \cdot py$ at 203 K is

Table 6
Vibrational data[a] for $WF_6 \cdot py$ and $WF_6 \cdot 2py$: comparison with those for pyridine (py)

Infared			Raman			Infrared			Raman		
py	$WF_6 \cdot py$	$WF_6 \cdot 2py$	py	$WF_6 \cdot py$	$WF_6 \cdot 2py$	py	$WF_6 \cdot py$	$WF_6 \cdot 2py$	py	$WF_6 \cdot py$	$WF_6 \cdot 2py$
	3780	3700	3173	3160	3220			1318			
	3730		3152	**3114**	3158	1292					
3150	3300		**3144**	**3104**	**3108**		1250	1247		1258	1254
	3120	**3120**		**3097**	3098	1215	**1227**	**1218**	**1215**	1224	1223
3085	3080	**3090**	3087	3086	3084						1194
				3078	3073						
			3067			**1145**	1165	1160	1145	1166	1162
											1152
3055			**3054**					1100		1104	1104
3030	3040	3040	**3022**	3042		1065	**1070**	**1065**	1067	1073	1075
3005	2970	3012	**2987**							**1048**	**1048**
2955	2930	2930	**2954**				1045	1040	**1030**	**1024**	**1026**
2910	2850	2840	2917			1027	**1020**	**1017**		**1014**	
2830	2715		2909			990	998	1002	**989**	998	
	2680	2640	2871			980	960	975	978	974	986
2600	2590		2830		2830	942		945	940	950	946
	2500	2490	2792					930			943
2450	2440		2705					905			
	2400		2657			884	880		880	860	
	2330	2310	2450			850	873	850			
2298	2270		2372			809			812		
2205	2230		2292		2328		**770**				
	2120					745	745	**753**	747		
	2033										
1988	1998	1990							714		
	1960	1965				700	707		707	**705***	
1920	1937	1940				675	**675***	**680***			
1870	1880	1913									
		1865								**660***	**661***
	1845	1845				650	**650***		651	642	636
1825	1825	1823					**635***			626	
1730	1725	1790				597		**598***	603	598	594
1685	1672	1700		1728			565	**560***		556	568
1633	1640	1660					543	508			483
	1615	1630					**465***	**460**		470*	
1598	1577	**1605**	1596	1614	1613			440*		447*	448*
1580	1540	1574	**1580**	1580	1582	403			406	435	
1573	1495	1540	**1572**					386	380	392	398
1480	1490	**1485**	1481	1494	1492			355*		365*	**368***
1437	**1460**	**1445**	1436				**330***	**337***		336*	**350***
1373	1402	1390					295*	287*		314*	338*
1355	1368	1360	1355				275*	252*		304*	304*
										283*	
										233*	242*
										200*	
										160*	**166***

[a] Frequencies in cm^{-1} with those of the most intense bands shown in bold. The main assignments for the py ligand given in Ref. [2] are also valid here. Asterisks indicate frequencies that are preferably assigned to the inorganic part of the adducts.

the same as that of WF_6. However, still in comparison with WF_6, at lower temperature the signal of the four equivalent F atoms was shifted to lower frequency, whereas that of the two other F atoms was shifted to higher frequency. This shows that in $WF_6 \cdot py$, in particular, the two F atoms opposite to the py ligand are not only less shielded than the four others, but also, quite surprisingly, less shielded than in the molecule WF_6.

The ^{19}F NMR data lead [14] to approximate values of the activation energy for internal fluorine exchange equal to 143 and 47 kJ mol^{-1} in $WF_6 \cdot 2py$ and $WF_6 \cdot py$, respectively. The origin of the fluorine exchange is not known: it may be due to traces of impurities such as

HF, it may result from the equilibria depicted in Eqs. (1) and (2), or may be first order and result from the interconversion of the F ligands through conformations close in energy. In the last case, the more hindered internal fluorine exchange observed for $WF_6 \cdot 2py$ compared with that for $WF_6 \cdot py$ would most probably originate from the intercalation of the W–N bonds between the two sets of W–F bonds (W–F(j), (j=1, 2), and W–F(k), (k=3, 4, 3^i, 4^i)).

3.4. Vibrational spectra

The frequencies observed for the infrared and Raman spectra of the adducts $WF_6 \cdot py$ and $WF_6 \cdot 2py$ are listed in Table 6. The frequencies attributable to the py ligand are comparable with those observed for the molecular adducts $WOF_4 \cdot py$ and $WOF_4 \cdot 2py$ [2]. The general tendency is towards an increase in frequency when compared with free py. As far as vibrations originating from WF_6 are concerned, the electron density conferred on the W atom by the N atom(s) results in a decrease of the W–F stretching frequencies. This is apparent for example in the Raman spectra in which the highest of these frequencies is located at 772, 705 and 661 cm^{-1} for WF_6 (crystal) [15], $WF_6 \cdot py$ and $WF_6 \cdot 2py$, respectively.

4. Conclusions

The product of the reaction of WF_6 with excess py has been shown both by ^{19}F NMR spectroscopy and X-ray diffraction to be an eight-coordinate tungsten(VI) fluoro adduct with a bicapped trigonal prismatic coordination geometry. The adduct $WF_6 \cdot py$ obtained with the reactants in stoichiometric amounts has also been shown by ^{19}F NMR spectroscopy to have a molecular structure derived from a trigonal prism but with only one of its square faces capped. The observed slightly higher stability of $WF_6 \cdot 2py$ (CN eight) relative to that of $WF_6 \cdot py$ (CN seven) is in the reverse order to that of $WOF_4 \cdot 2py$ (CN seven) and $WOF_4 \cdot py$ (CN six) [2]: in each case the hepta-coordinated adduct is the less stable.

5. Supplementary material

Tables of bond distances and bond angles, anisotropic thermal parameters, calculated positional parameters of H atoms, observed and calculated structure factors, and root-mean square amplitudes of thermal vibrations are available from the authors on request.

References

[1] D.L. Kepert, *Inorganic Stereochemistry*, Springer-Verlag, Berlin 1982, p. 117.

[2] L. Arnaudet, R. Bougon, B. Buu, P. Charpin, J. Isabey, M. Lance, M. Nierlich and J. Vigner, *Inorg. Chem., 28* (1989) 257.

[3] L. Arnaudet, R. Bougon, B. Buu, M. Lance, M. Nierlich and J. Vigner, *Inorg. Chem., 32* (1993) 1142.

[4] L. Arnaudet, R. Bougon, B. Buu, M. Lance, A. Navaza, M. Nierlich and J. Vigner, *J. Fluorine Chem., 67* (1994) 17.

[5] L. Arnaudet, R. Bougon, B. Buu, M. Lance, A. Navaza, M. Nierlich and J. Vigner, *J. Fluorine Chem., 59* (1992) 141.

[6] F.N. Tebbe and E.L. Muetterties, *Inorg. Chem., 7* (1968) 172.

[7] L. Arnaudet, R. Bougon, B. Buu, P. Charpin, J. Isabey, M. Lance, M. Nierlich and J. Vigner, *Can. J. Chem., 68* (1990) 507.

[8] L. Arnaudet, R. Bougon, B. Buu, M. Lance and W.C. Kaska, *J. Fluorine Chem., 53* (1991) 171.

[9] A.C.T. North, D.C. Phillips and F.S. Mathews, *Acta Crystallogr., A24* (1968) 351.

[10] C.K. Fair, MolEN; *An Interactive Intelligent System for Crystal Structure Analysis*, Enraf-Nonius, Delft, 1990.

[11] C.K. Johnson, Ortep II, *Report ORNL 5138*, Oak Ridge National Laboratory, Oak Ridge, TN, 1976.

[12] *International Tables for X-ray Crystallography*, Kynoch Press, Birmingham, UK, 1974, Vol. IV.

[13] SYBYL *Molecular Modeling Software*, Tripos Inc., St. Louis, MO, 1989, Vol. 5.2.

[14] J.A. Pople, W.G. Schneider and H.J. Bernstein, *High-resolution Nuclear Magnetic Resonance*, McGraw-Hill, New York, 1959, p. 339.

[15] E.R. Bernstein and G.R. Meredith, *J. Chem. Phys., 24* (1977) 289.